Electrochemical synthesis of ammonia from N_2 and H_2O based on $(Li,Na,K)_2CO_3$-$Ce_{0.8}Gd_{0.18}Ca_{0.02}O_{2-\delta}$ composite electrolyte and $CoFe_2O_4$ cathode

Ibrahim A. Amar[a,b], Christophe T.G. Petit[a], Gregory Mann[a], Rong Lan[a], Peter J. Skabara[b] and Shanwen Tao[a,*]

[a] Department of Chemical & Process Engineering, University of Strathclyde, Glasgow G1 1XJ, UK

[b] WestCHEM, Department of Pure & Applied Chemistry, University of Strathclyde, Glasgow G1 1XL, UK

ABSTRACT

Electrochemical synthesis of ammonia from water vapour and nitrogen was investigated using an electrolytic cell based on $CoFe_2O_4$-$Ce0.8Gd_{0.18}Ca_{0.02}O_{2-\delta}$ (CFO-CGDC), CGDC-ternary carbonate composite and $Sm_{0.5}Sr_{0.5}CoO_{3-\delta}$-$Ce_{0.8}Gd_{0.18}Ca_{0.02}O_{2-\delta}$ (SSCo-CGDC) as cathode, electrolyte and anode respectively. $CoFe_2O_4$, CGDC and SCCo were prepared via a combined EDTA-citrate complexing sol-gel and characterised by X-ray diffraction (XRD). The AC ionic conductivities of the CGDC-carbonate composite were investigated under three different atmospheres (air, dry O_2 and wet 5% H_2-Ar). A tri-layer electrolytic cell was fabricated by a cost-effective one-step dry-pressing and co-firing process. Ammonia was successfully synthesised from water vapour and nitrogen under atmospheric pressure and the maximum rate of ammonia production was found to be 6.5 $\times 10^{-11}$ mol s^{-1} cm^{-2} at 400 ºC and 1.6 V which is two orders of magnitude higher than that of previous report when ammonia was synthesised from N_2 and H_2O at 650 °C.

Keywords: Electrochemical synthesis of ammonia; water; nitrogen; spinels; co-doped ceria-carbonate composite electrolyte

---

* Corresponding author:
Department of Chemical & Process Engineering,
University of Strathclyde, Glasgow G1 1XJ, UK
Tel. +44 (0) 141 548 2361; Fax: +44 (0) 141 548 2539
E-mail: shanwen.tao@strath.ac.uk

1. Introduction

Ammonia (NH_3) is one of the most widely produced chemicals worldwide, and it is not only a major end product but also an important intermediate [1]. Ammonia is expected to play an important role in world future economy and its world production reached 136 million tons in 2011 [2]. In addition, ammonia has found a widespread use in many applications including; refrigeration, transportation, fertilisers (more than 80% of the produced ammonia) and other industries such as pharmaceuticals and explosives production [3-5]. Furthermore, ammonia is carbon-free at the end user stage and contains 17.6 wt% of hydrogen. Thus, ammonia is an interesting indirect hydrogen storage material [5]. The energy stored in ammonia can be recovered by direct ammonia fuel cells [5-7].

Presently, the predominant process for ammonia synthesis is Haber's process which involves the reaction of gaseous nitrogen and hydrogen on a Fe-based catalyst at 450-500 ºC under high pressure (150-300 bar). However, the main drawbacks of this process are; the low ammonia conversion (10-15%), severe environmental pollution due to CO_2 emission and high energy consumption [8]. To avoid the Haber's process limitations, several synthesis approaches constituting promising alternative methods to synthesise ammonia have been proposed. In 1998, Marnellos and Stoukides [9] demonstrated electrocatalytic ammonia synthesis for the first time using a solid oxide proton conductor (SCYb) under atmospheric pressure and high temperature. Over the porous palladium (Pd) cathode, gaseous H_2 and N_2 were converted into ammonia with a conversion greater than 78% at 570 °C. This means that by using solid state electrolytic cells, conversions are higher than those predicted by thermodynamic equilibrium and the requirements for high pressures are eliminated. Since then, several proton conductors have been utilised to synthesised ammonia [10-13]. Recently, the progress and the electrochemical synthesis of ammonia using solid state electrolytes has been reviewed [13, 14].

It is to be noted that pure H_2 was used in ammonia synthesis in the above mentioned reports. However, there are some problems associated with using H_2. These include; the production, purification, storage and transportation of hydrogen [15, 16]. On other hand, water is in

plentiful abundance and is therefore an ideal hydrogen source. Skodra and Stoukides [17] reported that ammonia was successfully synthesised for first the time from water and nitrogen rather than molecular hydrogen in an electrolytic cell based on either solid oxide protonic or oxygen ion conductors. Thus, using water instead of hydrogen is advantageous in that the costs of both the production and further purification of hydrogen will be eliminated. Furthermore, pure oxygen can be co-produced at minimal cost. The principle electrochemical synthesis of ammonia from water and N_2 using oxide-ion conductors (O^{2-}) can be written as follows [17]:

At the cathode,

$$3H_2O + N_2 + 6e^- \rightarrow 3O^{2-} + 2NH_3 \qquad (1)$$

At the anode, the transported oxygen ions through the electrolyte will combine to form oxygen gas:

$$3O^{2-} \rightarrow \tfrac{3}{2}O_2 + 6e^- \qquad (2)$$

Hence the overall reaction will be:

$$3H_2O + N_2 \rightarrow 2NH_3 + \tfrac{3}{2}O_2 \qquad (3)$$

In recent years, doped ceria-carbonate composite materials have drawn considerable interest owing to their potential applications as electrolytes for low/intermediate temperature (300-600 °C) fuel cells [18-23]. Another potential application for these materials include; water (steam) electrolysis [24], direct carbon fuel cells (DCFCs) [25, 26], electrochemical synthesis of ammonia [27] and carbon dioxide (CO_2) permeation membranes [28-30]. These materials exhibit high ionic conductivity (> 0.1 S cm^{-1}) below 600 °C which is higher that of pure doped ceria (10^{-2} S cm^{-1}) at 600 °C [20, 31]. As for the ionic conductivity of doped ceria, it has been reported that the ionic conductivity of Ca and Gd co-doped ceria (CGDC) is higher than that of single doped ceria [32]. In the literature, most investigations have been focused on composites based on doped ceria-binary carbonate systems (e.g., SDC-$(Li/Na)_2CO_3$) in which the binary carbonate melts at ~ 500 °C. On other hand, the melting point of the ternary carbonate ($(Li/Na/K)_2CO_3$, 43.5:31.5:25 mol%) is ~ 400 °C which is almost 100 °C lower than that of binary carbonate ($(Li/Na)_2CO_3$, 52:48 mol%) [33]. The lower working temperature of the ternary carbonate can minimise the thermal decomposition of produced ammonia.

Therefore, a combination between Ca and Gd co-doped ceria and the ternary ($(Li/Na/K)_2CO_3$ would result in a good composite electrolyte. In the present paper, a new composite electrolyte (CGDC-carbonate) has been synthesised and its application in the ammonia synthesis from water and nitrogen is investigated.

Cobalt-iron spinel oxides ($Co_xFe_{3-x}O_4$) are regarded as promising materials for application in many different technologies. In addition to the above mentioned properties, these materials are chemically and thermally stable [34]. These mixed transition metal oxides, in particular $CoFe_2O_4$, have exhibited great potential for application in gas sensors [35], heterogeneous catalysis such as the removal of NO_x [36] and the ammonia synthesis [37-39], and the electrocatalysis such as electrochemical reduction of NO_x [40], electrochemical synthesis of ammonia [41]and anode material for Li-ion batteries [42] etc. To the best of our knowledge, there is no report on the electrochemical synthesis of ammonia from H_2O and N_2 using $CoFe_2O_4$ as the catalyst.

2. Experimental

2.1 Materials synthesis

Ca and Gd co-doped ceria (CGDC) powder with a composition of ($Ce_{0.8}Gd_{0.18}Ca_{0.02}O_{2-\delta}$) was synthesised via a combined EDTA-citrate complexing sol-gel process [43]. Gadolinium oxide (Gd_2O_3, Alfa Aesar, 99.9 %), cerium nitrate hexahydrate ($Ce(NO_3)_3{\cdot}6H_2O$, Alfa Aesar, 99 %) and calcium nitrate tetrahydrate ($Ca(NO_3)_2{\cdot}4H_2O$, Alfa Aesar, 99 %) were used as starting materials. Gd_2O_3 was dissolved in diluted nitric acid to form gadolinium nitrate. Calculated amounts of $Ce(NO_3)_3{\cdot}6H_2O$ and $Ca(NO_3)_2{\cdot}4H_2O$ were dissolved in deionised water and mixed with gadolinium nitrate solution. Citric acid (Alfa Aesar, 99 %) and EDTA (ethylenediaminetetraacetic acid, Alfa Aesar, 99 %) were then added as complexing agents with a ratio of citric acid: EDTA: metal cations of 1.5:1:1. Dilute aqueous ammonia solution was then added to the mixed solution to adjust the pH value to around 6. Under heating and stirring, the solution was evaporated on a hot-plate, and then gradually changed into a brown sticky gel before complete drying leaving a porous and yellow ash. Finally, the resultant ash was grounded and subsequently calcined in air at 700 °C for 2 h with heating/cooling rates of 5 °C min^{-1} to obtain a single phase of CGDC.

$CoFe_2O_4$ (CFO) and $Sm_{0.5}Sr_{0.5}CoO_{3-\delta}$ (SSCo) were also synthesised via a combined EDTA-citrate complexing sol-gel process as described above. Samarium oxide (Sm_2O_3, Alfa Aesar, 99.9 %), strontium nitrate ($Sr(NO_3)_2$, Alfa Aesar, 99 %), ($Fe(NO_3)_3 \cdot 9H_2O$, Alfa Aesar, 98%) and cobalt nitrate ($Co(NO_3)_2 \cdot 6H_2O$, Sigma Aldrich, 98 + %) were used as starting materials. The resultant powders were grounded and subsequently calcined in air at 900 ºC for 3 h and 2 h with heating/cooling rates of 5 °C min^{-1} to obtain a single phase of CFO and SSCo respectively.

2.2 Preparation of the composite electrolyte

The ternary eutectic salt ($(Li/Na/K)_2CO_3$) was prepared by solid state reaction. Lithium carbonate (Li_2CO_3, Alfa Aesar, 98 %), sodium carbonate (Na_2CO_3, Aldrich, 99.5+ %) and potassium carbonate (K_2CO_3, Alfa Aesar, 99 %) were mixed with a molar ratio of 43.5:31.5:25 respectively. The mixture was ball milled in isopropanol for 9 h using a Pulverisette 6, Fritsch miller at speed of 400 rpm, and dried on a hot-plate, and then ground and calcined in air at 600 °C for 1h and quenched directly to room temperature.

The composite electrolyte CGDC-$(Li/Na/K)_2CO_3$ was also prepared by solid state reaction. The prepared CGDC powder was mixed with the ternary carbonate salt at weight ratio (70:30). The mixture was ball milled in isopropanol for 9 h. The material was fired in air at 600 °C for 1 h in sequence before being quenched to room temperature. The resultant mixture was dried and then ground thoroughly for subsequent use.

2.3 Materials Characterisation

X-ray diffraction (XRD) data were conducted at room temperature using a Panalytical X'Pert Pro diffractometer with a Ni-filter using Cu$K\alpha$ radiation using 40 kV and 40 mA (λ = 1.5405 Å), fitted with a X'Celerator detector. Absolute scans were recorded in the 2θ range 5-100º with a step size of 0.0167º.

Thermogravimetry and differential scanning calorimetry (TG/DSC) analyses were performed using a Stanton Redcroft STA/TGH series STA 1500 operating through a Rheometric Scientific system interface controlled by the software RSI Orchestrator. The thermal behaviour

of CFO cathode was studied in N_2 from room temperature to 500 ºC at a heating/cooling rate of 10 ºC/min.

The microstructures of the prepared catalyst and the cross-section of the single cell were examined using a Hitachi SU 6600 Scanning Electron Microscope (SEM).

The AC conductivity measurements for the composite electrolyte (CGDC-carbonate) were carried out using a computer-controlled Solartron Analytical 1470E unit controlled by Cell Test software for automatic data collection. The impedance spectra were recorded with an ac amplitude of 100 mV over the frequency range 1 MHz-0.01 Hz and 10 points per decades.

2.4 Pellets preparation

For ac conductivity measurements, the composite electrolyte powder was uniaxially dry-pressed at a pressure of 4 tons into pellets with diameter of 13 mm and thickness of ~ 2 mm. The green pellets were sintered in air at 700 ºC for 2 h at rate of 2 ºC heating/cooling. The Pellets were brushed onto both sides with Ag paste to serve as electrodes. The ac impedance measurements were preformed in three atmospheres namely; air, dry O_2 (dried through a solution of H_2SO_4 at 98%) and wet (~ 3% H_2O) 5% H_2-Ar. The measurements were made during the cooling cycle in the range of temperature 300-600 ºC.

A tri-layer single cell for ammonia synthesis was fabricated by a cost-effective one-step dry-pressing process. The anode material was a mixture of SSCo, CGDC and starch as the pore former in a weight ratio of 70:30:15 wt %. The cathode was made by mixing the CFO, CGDC and starch with a weight ratio of 70:30:15 wt %. The composite anode, composite electrolyte and composite cathode were fed into the die, layer by layer, with the aid of a sieve to ensure uniform powder distribution, and then uniaxially pressed at a pressure of 3.5 tons. The green pellet was sintered in air at 700 °C for 2 h. The catalyst surface area of the cathode was 0.785 cm^2. Silver paste was painted in a grid pattern on each electrode surface of the cell as a current collector. Ag wires were used as output terminals for both electrodes. It has been reported that silver itself have negligible catalytic effects on ammonia synthesis[17].

2.5 Ammonia synthesis

The fabricated single cells for ammonia synthesis were sealed onto a self-designed double chamber reactor using ceramic paste (Aremco, Ceramabond 552). The electrolytic cell constructed was as follows: air, SSCo-CGDC|CGDC-carbonate|CFO-CGDC, 3% H_2O-N_2. The cathode chamber was fed with 3%H_2O-N_2 (BOC), whereas the anode was exposed to air. The water vapour was supplied to the cathode chamber by bubbling a N_2 stream through a liquid water container, at 25°C. The DC potential was applied by a Solartron 1287A electrochemical interface controlled by CorrWare/CorrView software for automatic data collection. A direct potential was applied and the ammonia synthesised at the cathode chamber was absorbed by 20 ml of diluted HCl (0.01 M) for 30 min. The concentration of NH_4^+ in the absorbed solution was analysed using ISE (Thermo Scientific Orion Star A214). In situ AC impedance spectroscopy (IS) measurements were performed using a Schlumberger Solarton SI 1250 analyser coupled with a SI 1287 Electrochemical Interface controlled by Z-plot/Z-view software. The AC impedance spectra were recorded with an amplitude of 100 mV over the frequency range 65 kHz to 0.01 Hz.

3. Results and discussion

3.1 XRD, SEM and thermal analysis

The powder XRD patterns of the ternary carbonate, pure CGDC and CGDC-$(Li/Na/K)_2CO_3$ composite electrolytes are shown in Figures 1a-c. As can be seen from Figure 1a, the ternary carbonate which was calcined in air at 600 ºC for 1 h showed a complicated phase composition. A single phase CGDC with cubic fluorite structure was obtained after firing the CGDC precursor at 700 ºC in air for 2 h as illustrated in Figure 1b. Figure 1c represents the XRD pattern of CGDC-carbonate composite calcined in air at 600 ºC for 1 h and quenched directly to room temperature. As can be seen the major peaks could be ascribed to the pure CGDC phase, indicating that the ternary carbonates in the composite electrolyte are present in the amorphous phase. The crystallite size of pure CGDC is ~ 21.03 nm, while that of the CGDC-carbonate composite is ~ 24.49 nm, estimated from Sherrer's formula.

Figures 3207a-d show the XRD patterns of pure CFO (JCPDS No 00-022-1086), CFO-CGDC composite cathode, pure SSCo and SSCo-CGDC composite anode. As can be seen a single phase of spinel (CFO) was obtained after firing the precursor in air at 900 ºC for 3 h (Figure 2. Room temperature XRD patterns of:; (a) CFO calcined in air at 900 ºC for 3 h; (b) CFO-CGDC

composite cathode fired in air at 700 ºC; (c) SSCo calcined in air at 900 ºC for 2 h; (d) SSCo-CGDC composite anode fired in air at 700 ºC.a). Figure 2. Room temperature XRD patterns of:; (a) CFO calcined in air at 900 ºC for 3 h; (b) CFO-CGDC composite cathode fired in air at 700 ºC; (c) SSCo calcined in air at 900 ºC for 2 h; (d) SSCo-CGDC composite anode fired in air at 700 ºC.b represents the XRD pattern of the composite cathode (CFO-CGDC, 70:30 wt %), and only peaks corresponding to CFO and CGDC were found indicating good chemical compatibility between the cathode compositions at the single cell sintering temperature. The XRD patterns of SSCo and the composite anode (SSCo-CGDC, 70:30 wt %) are shown in Figure 2. Room temperature XRD patterns of:; (a) CFO calcined in air at 900 ºC for 3 h; (b) CFO-CGDC composite cathode fired in air at 700 ºC; (c) SSCo calcined in air at 900 ºC for 2 h; (d) SSCo-CGDC composite anode fired in air at 700 ºC.c and d respectively. As can be seen, the single phase perovskite oxide of SSCo was obtained by calcining in air at 900 ºC for 2 h. The composite anode (SSCo-CGDC) shows only the peaks corresponding to SSCo and CGDC indicating good chemical compatibility between the anode compositions at the cell sintering temperature. The crystallite size of pure CFO is ~ 47.69 nm, while that of SSCo is ~ 27.30 nm, estimated from Sherrer's formula. The microstructures of CFO powder calcined in air at 900 ºC for 3 h was investigated by SEM, as shown in **Error! Reference source not found.**. As can be seen, the catalyst morphology consists of large grains surrounded by small homogenous primary grain particles and many pores.

The thermal behaviour of CFO cathode was investigated under N_2 as the cathode is exposed to the gas during the ammonia synthesis. Figure 3a shows TGA-DSC curves of the CFO cathode in N_2 atmosphere from room temperature up to 500 °C at a rate of 10 °C/min. In the range of room temperature to 200 ºC, a small endothermic peak at 78 ºC was observed accompanied by a weight loss of about 0.28 %, which could be attributed to the loss of absorbed water. Between 200-500 ºC, no significant weight loss was observed and the total weight loss was about 0.37 %. The DSC curve shows no obvious thermal effects indicating that there are no phase transitions or sample decomposition and there is no reaction between CFO and N_2 in the measured temperature range. This suggests that the CFO cathode is thermally and chemically stable in N_2 within the measured temperature range. In order to confirm the thermal stability of the cathode under a N_2 atmosphere, an XRD analysis was carried out after thermal analysis measurements and the XRD pattern is shown Figure 3b. As can be seen, the oxide retains the same spinal structure indicating the thermal stability of CFO cathode under a N_2 atmosphere in the measured temperature range.

3.2 Conductivity of the composite electrolyte

The ionic conductivities of the composite electrolyte (CGDC-carbonate) were investigated under three different atmospheres (air, dry O_2 and wet 5% H_2-Ar) as shown in Figure 4. It is to be noted that since the bulk and grain boundary contributions cannot be separated, only the total conductivity was measured. As can be seen, the ionic conductivities of the composite electrolyte increase with an increase in the operating temperature in all atmospheres under investigation. In addition, it can be clearly noticed that the conductivities changed at two different regions below and above ~ 375 ºC which is ~ 25 ºC lower than the melting point of the ternary carbonate (~ 397 ºC) [33]. Such conductivity jump phenomena above the carbonate melting point have been observed for a doped ceria-ternary carbonate composite (SDC-$(Li/Na/K)_2CO_3$) [23] and a doped ceria-binary carbonate composite (e.g., SDC- or GDC-$(Li/Na)_2CO_3$) [44, 45]. Within the range of temperature 600-400 ºC, the total conductivities were 0.49-0.12 S cm^{-1}, 0.50-0.13 S cm^{-1} and 0.52-0.13 S cm^{-1} in air, dry O_2 and wet 5% H_2-Ar respectively. These values are higher than that of pure CGDC (7.42×10^{-2} S cm^{-1}) at 700 ºC and GDC-carbonate composite (0.22 S cm^{-1}) at 600 ºC [32, 45]. The apparent activation energies (E_a) of the composite electrolyte at high temperature (600-400 ºC) under different atmospheres were extracted from the slope of each series of points in the Arrhenius plots of conductivity as shown in the inset of Figure 4. The activation energies were found to be 0.42 ± 0.08 eV, 0.40 ± 0.07 eV and 0.40 ± 0.06 eV for the composite electrolyte in air, dry O_2 and wet 5% H_2-Ar respectively. At low temperature (375-300 ºC), the ionic conductivities of the composite electrolyte dropped significantly and were found to be 6.74×10^{-2}-5.41×10^{-6}, 8.99×10^{-2}-2.99×10^{-5} and 0.11-1.21×10^{-3} S cm^{-1} in air, dry O_2 and wet 5% H_2-Ar respectively. At lower temperature, the conductivity in 5%H_2/Ar is slightly higher indicating proton conduction which was also previously observed by another research group [46]. It should be noted that the measured total conductivity includes all possible mobile ions such as Li^+, Na^+, K^+, H^+, HCO_3^-, CO_3^{2-}, O^{2-}. It is presumed that the electronic conduction of the oxide-carbonate composite is negligible as high open circuit voltage was observed in fuel cells based on oxide-carbonate electrolyte[47, 48].

3.3 Ammonia synthesis at different temperatures

Figure 5 shows the electrolytic cell performance stabilities during the synthesis of ammonia at different temperatures (375-450 °C) with an applied voltage of 1.4 V over a period of 30 min. It is to be noted that the electrolytic cell demonstrated stable performance at all temperature under investigation. Furthermore, the generated current densities increased with an increase in the cell operating temperature and reached a maximum value of 23.14 mA cm^{-2} at 450 °C. This increase of current densities with temperature could also be explained by an increase in the ionic conductivity of the working electrolyte which means that more O^{2-} was transported through the electrolyte to the anode surface.

The AC impedance spectra of the electrolytic cell based on the CFO-CGDC composite cathode at different temperatures (375-450 °C) under open circuit conditions are shown in Figure 6. As can be seen from Figure 6a, the spectra are composed of two depressed semicircles, suggesting that there are at least two electrode processes. The impedance date were fitted using Zview software with an equivalent circuit model of the type LRs(R1CPE1)(R2CPE2) as shown in Figure 6b. In this circuit L is an inductance that originated from the electrochemical equipment and connection wires, Rs is the series resistance associated with the overall cell resistance including; electrolyte, electrodes, and contact resistances. The two components (R1CPE1) and (R2CPE2) in series are associated with the electrode processes at high and low frequency arcs respectively (R = resistance, CPE = constant phase element). It can be also seen from Figure 7, the Rs resistance, which is mainly related to the ohmic resistance of the electrolyte, decreased significantly as the cell operating temperature increased from 375 to 450 °C. This could be attributed to the enhancement in the ionic conductivity of the composite electrolyte as the operating temperature is increased. There was also a significant decrease in the total polarisation resistance (Rp) which is the sum of R1 and R2, with an increase in operating temperature, which could be due to the improvement in the catalytic activity of the cathode with temperature.

The effect of the operating temperature on the rate of ammonia formation was investigated by varying the cell temperature from 375 °C to 450 °C and keeping the applied potential at a constant value of 1.4 V. As can be seen from Figure 7, the rate of ammonia formation increased markedly with an increase in the operating temperature and reached a maximum value of 3.99 $\times 10^{-11}$ mol s^{-1} cm^{-2} at 400 °C. This ammonia formation rate corresponds to current density and current efficiency of 12.22 mA cm^{-2} and 0.095 % respectively. The increase in the rate of

ammonia formation with temperature could also be related to the increase in the ionic conductivity as mentioned above. On the other hand, a decrease in the rate of ammonia formation was observed by further increasing the operating temperature, although the ionic conductivity of the working electrolyte increases with this latter parameter. This could be attributed to thermal decomposition of ammonia which becomes faster than the rate of ammonia formation at high temperature. Similar phenomenon was also observed in a previous report [27]. It should be noted that the change in catalytic activity of cathode due to microstructure change in relation to melting of carbonates cannot be ruled out. The stability of ternary $(Li,Na,K)_2CO_3$ carbonate has been investigated by Olivares et al. and it was found the melt is stable in air up to 530 °C[49]. Therefore an operating temperature above 530 °C should be avoided.

In the Haber-Bosch process, the presence of ppm level oxygen may poison the commonly used Fe-based catalysts. In industry, extensive purification of N_2 and H_2 is needed and this remarkably increases the overall cost of the process [50, 51]. In the present study, the generated oxygen ions at the cathode side will be transported to the anode side. Since the composite cathode (CFO-CGDC) is a mixed electronic and ionic conductor, the oxygen ions will transport through CGDC to the composite electrolyte and then reach the anode/electrolyte interface and combine forming an oxygen gas as expressed by reaction (2). Oxygen is not formed at the cathode thus will not further poison that catalysts.

3.4 Ammonia synthesis at different applied voltages

Figure 8 represents the performance of the electrolytic cell at constant temperature and different applied voltages over a period of 30 min. It is important to note that the generated current densities remain almost constant at all applied voltages, indicating a stable electrochemical process. In addition, the highest current density (12.28 mA cm^{-2}) was observed when the electrolytic cell was operated with an applied voltage of 1.8 V. A higher applied dc voltage did not result in higher current, which may be related to the 'blocking effect' of Li^+, Na^+ and K^+ ions. These ions may form a positively charged layer on the electrolyte side at the cathode/electrolyte interface thus partially blocking the transfer of the protons or O^{2-} ions. A similar phenomenon was also observed in the electrochemical synthesis of ammonia based on a $Li^+/H^+/NH_4^+$ conducting electrolyte [52].

Since the highest rate of ammonia formation was obtained when the electrolytic cell operated at 400 °C, the effect of the applied voltage on the rate of ammonia formation has been

investigated under this working temperature. As can be seen from Figure 9, the rate ammonia formation increased slightly with an increase in the applied voltage from 1.2 V to 1.4 V. However, a significant rate increase was observed with an applied voltage of 1.6 V (6.5×10^{-11} mol s^{-1} cm^{-2}). On other hand, the rate of ammonia formation dropped significantly by increasing the applied voltage. This could be ascribed to competitive adsorption between N_2 and H_2 over the cathode surface [53]. It is to be noted that the value of 6.49×10^{-11} mol s^{-1} cm^{-2} represents the highest rate of ammonia formation and 1.6 V is the optimum applied voltage for this study. This rate corresponds to current density and efficiency of 11.28 mA/cm^2 and 0.17 % respectively. This low current efficiency indicates the there is more than one process occurring at the cathode surface and the competitive hydrogen evolution reaction is the dominant one. Although the rate of ammonia formation was low, this value is two orders of magnitude higher than that reported previously (3.75×10^{-13} mol s^{-1} cm^{-2} at 650 °C) when steam and N_2 were used to produce ammonia in an electrolytic cell based on an oxide ion conducting electrolyte (O^{2-}) and a Ru-based cathode [17]. The difference is likely due to the various operating temperatures. This indicates that a lower operating temperature may minimise thermal decomposition and benefit the formation of ammonia.

Figure 11a shows the microstructure of the cross-sectional area of a single cell (before testing) based on the CFO-CGDC composite cathode, sintered in air at 700 ºC for 2 h. As can be seen, the sintered cell shows good adhesion at the interfaces between the porous electrodes (anode and cathode) and the dense electrolyte (CGDC-carbonate composite). Figure 11b shows the microstructure of the cross-sectional area of the single cell sintered after ammonia synthesis (i.e. after testing). No obvious change in morphology was observed after testing and the cell is still in good condition (Figure 11c-d).

4. Conclusion

$CoFe_2O_4$ (CFO), $Ce_{0.8}Gd_{0.18}Ca_{0.02}O_{2-\delta}$ (CGDC) and $Sm_{0.5}Sr_{0.5}CoO_{3-\delta}$ (SSCo) were prepared via a combined EDTA-citrate complexing sol-gel process. The composite electrolytes was prepared by mixing $Ce_{0.8}Gd_{0.18}Ca_{0.02}O_{2-\delta}$ with the ternary carbonate (70: 30 wt %). The ionic conductivities of the composite electrolyte within the temperature range of 600-400 ºC were 0.49-0.12 S cm^{-1}, 0.50-0.13 S cm^{-1} and 0.52-0.13 S cm^{-1} in air, dry O_2 and wet 5% H_2-Ar respectively. A tri-layer electrolytic cell was successfully fabricated by a cost effective one-

step dry-pressing and co-firing process. Ammonia was successfully synthesised from water (3% H_2O) and nitrogen under atmospheric pressure using SSCO-CGDC, CGDC-(Li/Na/K)$_2CO_3$ and CFO-CGDC composites as anode, electrolyte and cathode respectively. The maximum rate of ammonia production was found to be 6.5×10^{-11} mol s^{-1} cm^{-2} at 400 ºC and 1.6 V which is two orders of magnitude higher than that of previous report when ammonia was synthesised from N_2 and H_2O at 650 °C.

Acknowledgements

The authors thank EPSRC SuperGen XIV 'Delivery of Sustainable Hydrogen' project (Grant No EP/G01244X/1) for funding. One of the authors (Amar) thanks The Libyan Cultural Affairs, London for financial support of his study in UK.

References

[1] Slack A, James G. Ammonia.(In four parts) Fertilizer Science and Technology Series, Vol. 2. New York: Marcel Dekker, Inc; 1973.
[2] US, Survey G. Mineral Commodity Summaries: Geological Survey; 2012.
[3] Douglas J. Synthesis of ammonia, The Macmillan Press Ltd., New York; 1971.
[4] Zamfirescu C, Dincer I. Using ammonia as a sustainable fuel. J. Power Sources. 2008;185:459-65.
[5] Lan R, Irvine JTS, Tao SW. Ammonia and related chemicals as potential indirect hydrogen storage materials. Inter. J. Hydrogen Energy. 2012;37:1482-94.
[6] Lan R, Tao SW. Direct ammonia alkaline anion-exchange membrane fuel cells. Electrochem. & Solid-State Lett. 2010;13:B83-B6.
[7] Alagharu V, Palanki S, West KN. Analysis of ammonia decomposition reactor to generate hydrogen for fuel cell applications. J. Power Sources. 2010;195:829-33.
[8] Appl M. Ammonia: principles and industrial practice: Wiley-VCH Weinheim, Germany; 1999.
[9] Marnellos G, Stoukides M. Ammonia synthesis at atmospheric pressure. Science. 1998;282:98-100.
[10] Xie YH, Wang JD, Liu RQ, Su XT, Sun ZP, Li ZJ. Preparation of $La_{1.9}Ca_{0.1}Zr_2O_{6.95}$ with pyrochlore structure and its application in synthesis of ammonia at atmospheric pressure. Solid State Ionics. 2004;168:117-21.
[11] Li ZJ, Liu RQ, Xie YH, Feng S, Wang JD. A novel method for preparation of doped $Ba_3Ca_{1.18}Nb_{1.82}O_{9-\delta}$: Application to ammonia synthesis at atmospheric pressure. Solid State Ionics. 2005;176:1063-6.
[12] Wang W, Cao X, Gao W, Zhang F, Wang H, Ma G. Ammonia synthesis at atmospheric pressure using a reactor with thin solid electrolyte $BaCe_{0.85}Y_{0.15}O_{3-\alpha}$ membrane. J. Memb. Sci. 2010;360:397-403.
[13] Giddey S, Badwal SPS, Kulkarni A. Review of electrochemical ammonia production technologies and materials. Inter. J Hydrogen Energy. 2013;38:14576-94.
[14] Amar IA, Lan R, Petit CT, Tao SW. Solid-state electrochemical synthesis of ammonia: a review. J. Solid State Electrochem. 2011;15:1845-60.
[15] Wang K, Ran R, Shao Z. Methane-fueled IT-SOFCs with facile in situ inorganic templating synthesized mesoporous $Sm_{0.2}Ce_{0.8}O_{1.9}$ as catalytic layer. J. Power Sources. 2007;170:251-8.
[16] McIntosh S, Gorte RJ. Direct hydrocarbon solid oxide fuel cells. Chem. Rev.-Columbus. 2004;104:4845-66.
[17] Skodra A, Stoukides M. Electrocatalytic synthesis of ammonia from steam and nitrogen at atmospheric pressure. Solid State Ionics. 2009;180:1332-6.
[18] Li X, Zhao H, Shen W, Gao F, Huang X, Li Y, et al. Synthesis and properties of Y-doped SrTiO3 as an anode material for SOFCs. J Power Sources. 2007;166:47-52.
[19] Zhang L, Lan R, Xu X, Tao S, Jiang Y, Kraft A. A high performance intermediate temperature fuel cell based on a thick oxide-carbonate electrolyte. J. Power Sources. 2009;194:967-71.
[20] Wang X, Ma Y, Raza R, Muhammed M, Zhu B. Novel core-shell SDC/amorphous Na2CO3 nanocomposite electrolyte for low-temperature SOFCs. Electrochem. Comm. 2008;10:1617-20.
[21] Raza R, Wang X, Ma Y, Zhu B. Study on calcium and samarium co-doped ceria based nanocomposite electrolytes. J. Power Sources. 2010;195:6491-5.

[22] Wang X, Ma Y, Li S, Kashyout A-H, Zhu B, Muhammed M. Ceria-based nanocomposite with simultaneous proton and oxygen ion conductivity for low-temperature solid oxide fuel cells. J. Power Sources. 2011;196:2754-8.
[23] Xia C, Li Y, Tian Y, Liu Q, Zhao Y, Jia L, et al. A high performance composite ionic conducting electrolyte for intermediate temperature fuel cell and evidence for ternary ionic conduction. J. Power Sources. 2009;188:156-62.
[24] Zhu B, Albinsson I, Andersson C, Borsand K, Nilsson M, Mellander B-E. Electrolysis studies based on ceria-based composites. Electrochem. Comm. 2006;8:495-8.
[25] Liu Q, Tian Y, Xia C, Thompson LT, Liang B, Li Y. Modeling and simulation of a single direct carbon fuel cell. J. Power Sources. 2008;185:1022-9.
[26] Li H, Liu Q, Li Y. A carbon in molten carbonate anode model for a direct carbon fuel cell. Electrochim. Acta. 2010;55:1958-65.
[27] Amar IA, Petit CT, Zhang L, Lan R, Skabara PJ, Tao SW. Electrochemical synthesis of ammonia based on doped-ceria-carbonate composite electrolyte and perovskite cathode. Solid State Ionics. 2011;201:94-100.
[28] Li Y, Rui Z, Xia C, Anderson M, Lin YS. Performance of ionic-conducting ceramic/carbonate composite material as solid oxide fuel cell electrolyte and CO_2 permeation membrane. Catal. Today. 2009;148:303-9.
[29] Wade JL, Lee C, West AC, Lackner KS. Composite electrolyte membranes for high temperature CO2 separation. J. Memb. Sci. 2011;369:20-9.
[30] Zhang L, Xu N, Li X, Wang S, Huang K, Harris W, et al. High CO_2 permeation flux enabled by highly interconnected three-dimensional ionic channels in selective CO_2 separation membranes. Energy & Environ. Sci. 2012;5:8310-7
[31] Fu YP, Chen SH, Huang JJ. Preparation and characterization of $Ce_{0.8}M_{0.2}O_2$ (M=Y, Gd, Sm, Nd, La) solid electrolyte materials for solid oxide fuel cells. Inter. J. Hydrogen Energy. 2010;35:745-52.
[32] Zhao X-L, Liu J-J, Xiao T, Wang J-C, Zhang Y-X, Yao H-C, et al. Effect of Ca co-dopant on the electrical conductivity of Gd-doped ceria. J. Electroceram. 2012;28:149-57.
[33] Janz GJ, Lorenz MR. Solid-liquid phase equilibria for mixtures of lithium, sodium, and potassium carbonates. J. Chem. & Eng. Data. 1961;6:321-3.
[34] Tong J, Bo L, Li Z, Lei Z, Xia C. Magnetic CoFe2O4 nanocrystal: A novel and efficient heterogeneous catalyst for aerobic oxidation of cyclohexane. J. Molecular Catal. A: Chem. 2009;307:58-63.
[35] Bodade AB, Bodade AB, Wankhade H, Chaudhari G, Kothari D. Conduction mechanism and gas sensing properties of $CoFe_2O_4$ nanocomposite thick films for H_2S gas. Talanta. 2012;89:183-8.
[36] Fino D, Russo N, Saracco G, Specchia V. Catalytic removal of NO_x and diesel soot over nanostructured spinel-type oxides. J. Catal. 2006;242:38-47.
[37] Wang W-X, Zhao H-Q, Du B-S, Wen J-M, Li F, Wang D-M. Activity and reduction behavior of fused iron catalysts containing cobalt for ammonia synthesis: a structure study. Appl. Catal. A: General. 1995;122:5-20.
[38] Rajaram RR, Sermon PA. Adsorption and catalytic properties of $Co_xFe_{3-x}O_4$ spinels. Part 1.—Preparation and characterisation of precursors to ammonia-synthesis catalysts. J Chem Soc, Faraday Trans 1. 1985;81:2577-91.
[39] Rajaram RR, Sermon PA. Adsorption and catalytic properties of $Co_xFe_{3-x}O_4$ spinels. Part 2.—Hydrogen chemisorption on precursors to ammonia synthesis catalysts. J Chem Soc, Faraday Trans 1. 1985;81:2593-603.
[40] Simonsen VLE, Lilliedal M, Petersen R, Kammer K. Spinels as cathodes for the electrochemical reduction of O_2 and NO. Topics in Catal. 2007;45:143-8.

[41] Amar IA, Lan R, Petit CTG, Arrighi V, Tao SW. Electrochemical synthesis of ammonia based on a carbonate-oxide composite electrolyte. Solid State Ionics. 2011;182:133-8.
[42] Vidal-Abarca C, Lavela P, Tirado JL. On the role of faradaic and capacitive contributions in the electrochemical performance of $CoFe_2O_4$ as conversion anode for Li-ion cells. Solid State Ionics. 2010;181:616-22.
[43] Gao Z, Mao Z, Wang C, Huang J, Liu Z. Composite electrolyte based on nanostructured Ce0. 8Sm0. 2O1. 9 (SDC) for low temperature solid oxide fuel cells. Inter. J. Energy Res. 2009;33:1138-44.
[44] Huang J, Mao Z, Liu Z, Wang C. Development of novel low-temperature SOFCs with co-ionic conducting SDC-carbonate composite electrolytes. Electrochem. Comm. 2007;9:2601-5.
[45] Chockalingam R, Basu S. Impedance spectroscopy studies of Gd-CeO_2-(LiNa)CO_3 nano composite electrolytes for low temperature SOFC applications. Inter. J. Hydrogen Energy. 2011;36:14977-83.
[46] Rondao AIB, Patricio SG, Figueiredo FML, Marques FMB. Role of gas-phase composition on the performance of ceria-based composite electrolytes. Inter. J. Hydrogen Energy. 2013;38:5497-506.
[47] Fan L, Wang C, Chen M, Zhu B. Recent development of ceria-based (nano)composite materials for low temperature ceramic fuel cells and electrolyte-free fuel cells. J. Power Sources. 2013;234:154-74.
[48] Zhang L, Lan R, Kraft A, Tao SW. A stable intermediate temperature fuel cell based on doped-ceria–carbonate composite electrolyte and perovskite cathode. Electrochem. Comm. 2011;13:582-5.
[49] Olivares RI, Chen C, Wright S. The Thermal Stability of Molten Lithium-Sodium-Potassium Carbonate and the Influence of Additives on the Melting Point. J. Solar Energy Eng.-Trans Asme. 2012;134.
[50] Waugh KC, Butler D, Hayden BE. The mechanism of the poisoning of ammonia-synthesis catalysts by oxygenates O_2, CO and H_2O - an in-situ method for active surface determination. Catal. Lett. 1994;24:197-210.
[51] Jennings J. Catalytic ammonia synthesis: fundamentals and practice: Springer; 1991.
[52] Lan R, Tao SW. Electrochemical synthesis of ammonia directly from air and water using a $Li^+/H^+/NH_4^+$ mixed conducting electrolyte. RSC Adv. 2013;3:18016-21.
[53] Sclafani A, Augugliaro V, Schiavello M. Dinitrogen electrochemical reduction to ammonia over Iron cathode in aqueous medium. J. Electrochem. Soc. 1983;130:734-6.

Captions

Figure 1. XRD patterns of; (a) $(Li/Na/K)_2CO_3$ calcined in air at 600 ºC for 1 h, (b) CGDC calcined in air at 700 ºC for 2 h, (c) CGDC-$(Li/Na/K)_2CO_3$ (70:30 wt%) calcined in air at 600 ºC for 1 h.

Figure 2. Room temperature XRD patterns of:; (a) CFO calcined in air at 900 ºC for 3 h; (b) CFO-CGDC composite cathode fired in air at 700 ºC; (c) SSCo calcined in air at 900 ºC for 2 h; (d) SSCo-CGDC composite anode fired in air at 700 ºC.Figure 2. Scanning electron micrograph of CFO cathode calcined in air at 900 °C for 3 h.

Figure 3. (a) TGA-DSC curve of CFO in nitrogen up to 500 ºC; (b) XDR pattern of CFO after thermal analysis.

Figure 4. Conductivity plot against temperature of CGDC-$(Li/Na/K)_2CO_3$ composite.

Figure 5. Electrolytic cell performance stability at 1.4 V and 375-450 °C. The electrolytic cell was; air, SSCo-CGDC|CGDC-carbonate|CFO-CGDC, 3% H_2O-N_2.

Figure 6. (a) Impedance spectra under open circuit condition of the cell based on CFo-CGDC composite cathode at 375-450 °C; (b) an equivalent circuit for the impedance data.

Figure 7. Dependence of the rate of ammonia formation on the operating temperature. The electrolytic cell was; air, SSCo-CGDC|CGDC-carbonate|CFO-CGDC, 3% H_2O-N_2.

Figure 8. Electrolytic cell performance stability at 400 °C and under different voltages (1.2-1.8 V).The electrolytic cell was; air, SSCo-CGDC|CGDC-carbonate|CFO-CGDC, 3% H_2O-N_2.

Figure 9. Dependence of the rate of ammonia formation on the applied voltage at 400 °C. The electrolytic cell was: air, SSCo-CGDC|CGDC-carbonate|CFO-CGDC, 3% H_2O-N_2.

Figure 11. Cross-sectional scanning electron micrographs of the single cell. (a) before ammonia synthesis; (b) after ammonia synthesis experiments; (c) interface between cathode and electrolyte after ammonia synthesis

experiments; (d) interface between electrolyte and anode after ammonia synthesis experiments.

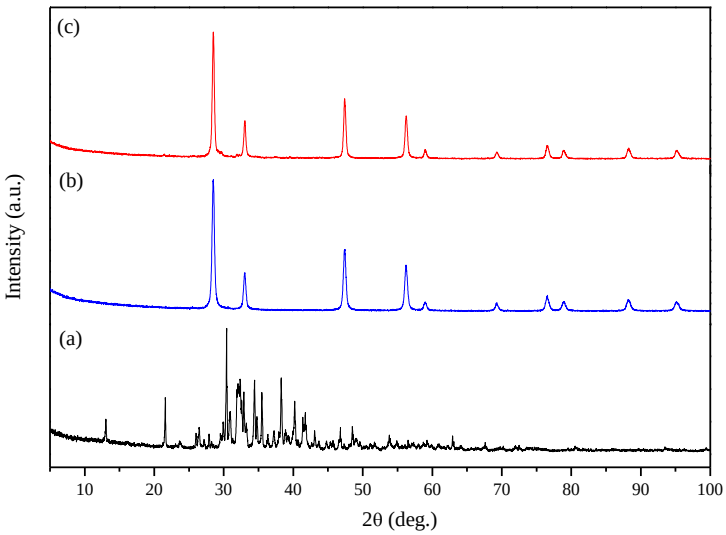

Figure 1. XRD patterns of; (a) $(Li/Na/K)_2CO_3$ calcined in air at 600 ºC for 1 h, (b) CGDC calcined in air at 700 ºC for 2 h, (c) CGDC-$(Li/Na/K)_2CO_3$ (70:30 wt%) calcined in air at 600 ºC for 1 h.

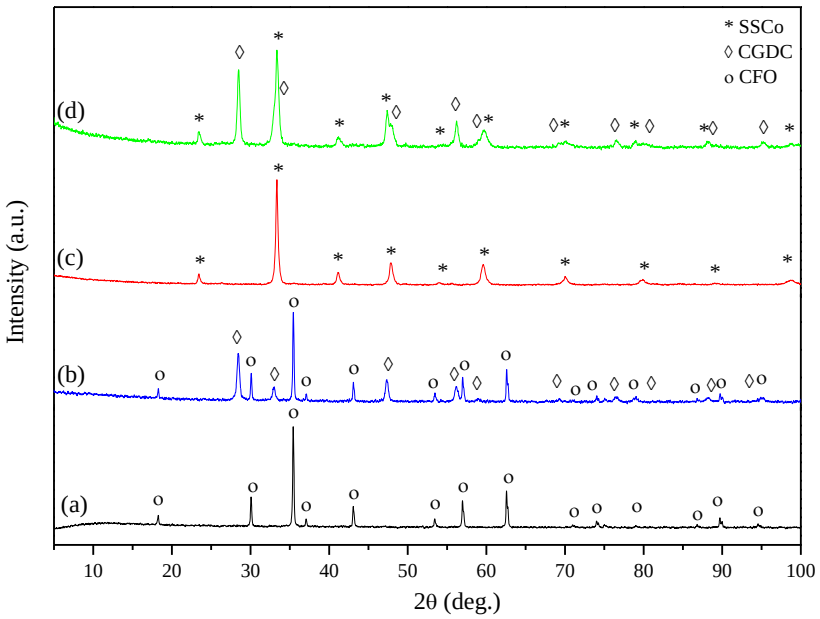

Figure 2. Room temperature XRD patterns of:; (a) CFO calcined in air at 900 ºC for 3 h; (b) CFO-CGDC composite cathode fired in air at 700 ºC; (c) SSCo calcined in air at 900 ºC for 2 h; (d) SSCo-CGDC composite anode fired in air at 700 ºC.

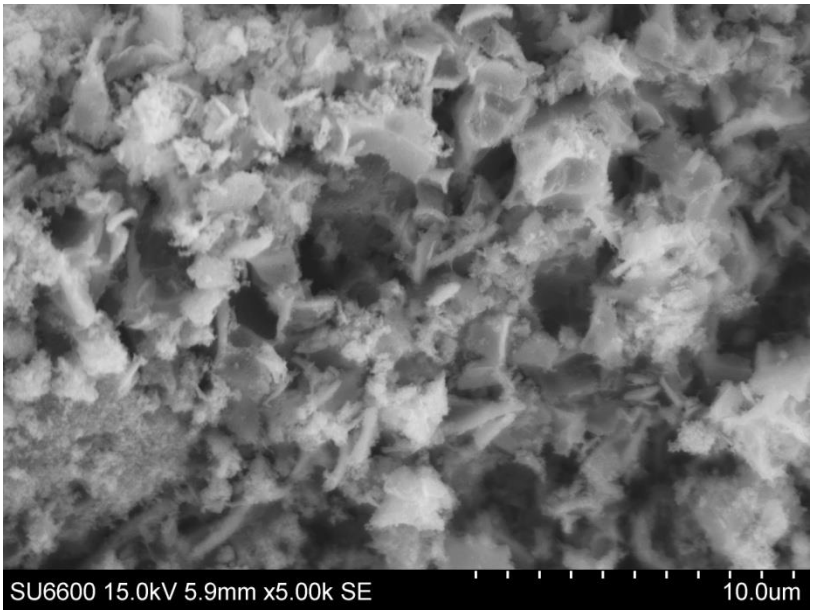

Figure 2. Scanning electron micrograph of CFO cathode calcined in air at 900 °C for 3 h.

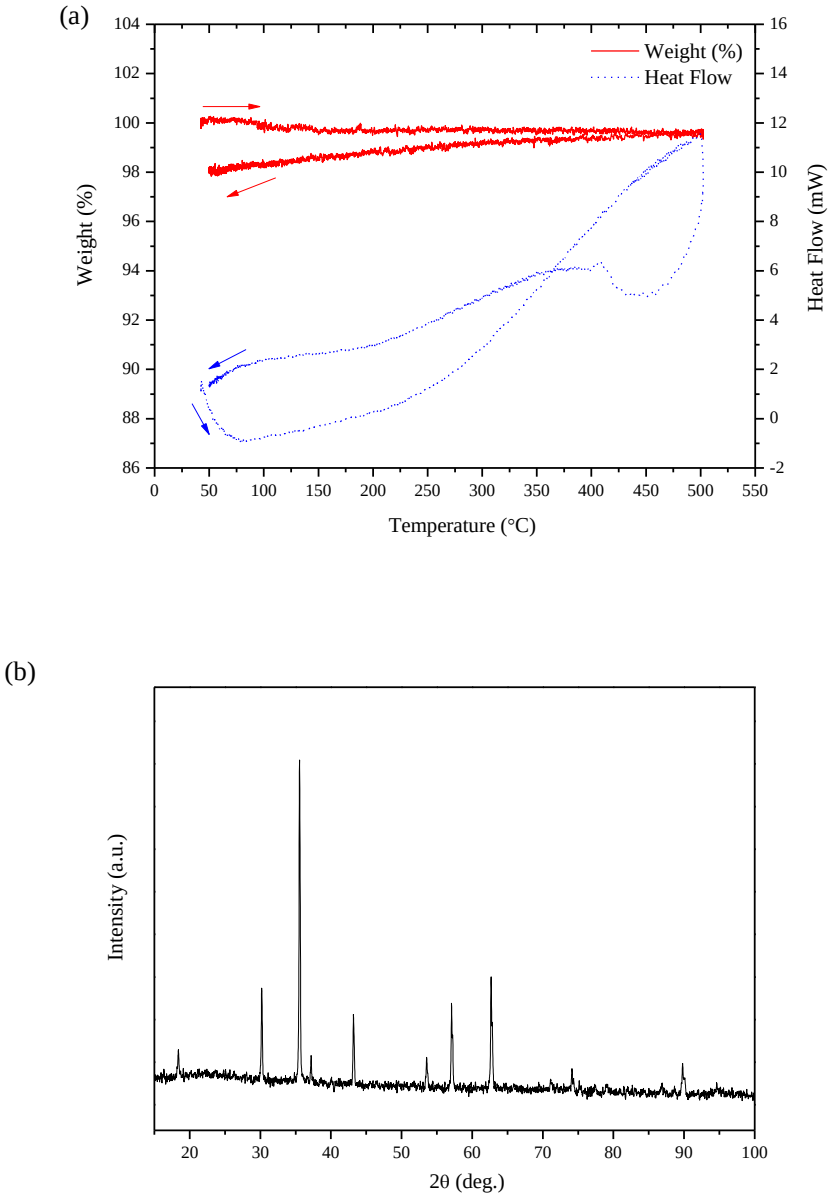

Figure 3. (a) TGA-DSC curve of CFO in nitrogen up to 500 ºC; (b) XDR pattern of CFO after thermal analysis.

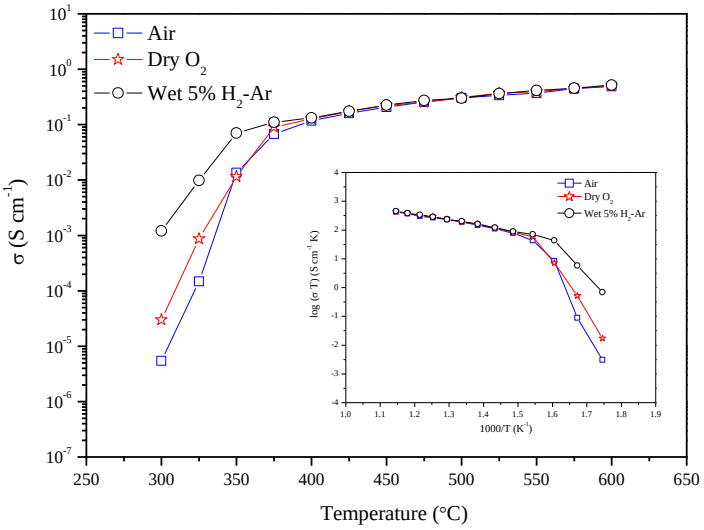

Figure 4. Conductivity plot against temperature of CGDC-(Li/Na/K)$_2$CO$_3$ composite.

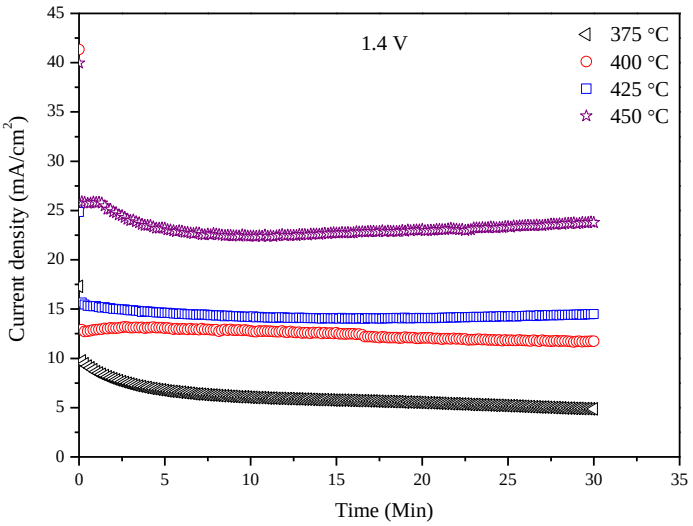

Figure 5. Electrolytic cell performance stability at 1.4 V and 375-450 °C. The electrolytic cell was; air, SSCo-CGDC|CGDC-carbonate|CFO-CGDC, 3% H_2O-N_2.

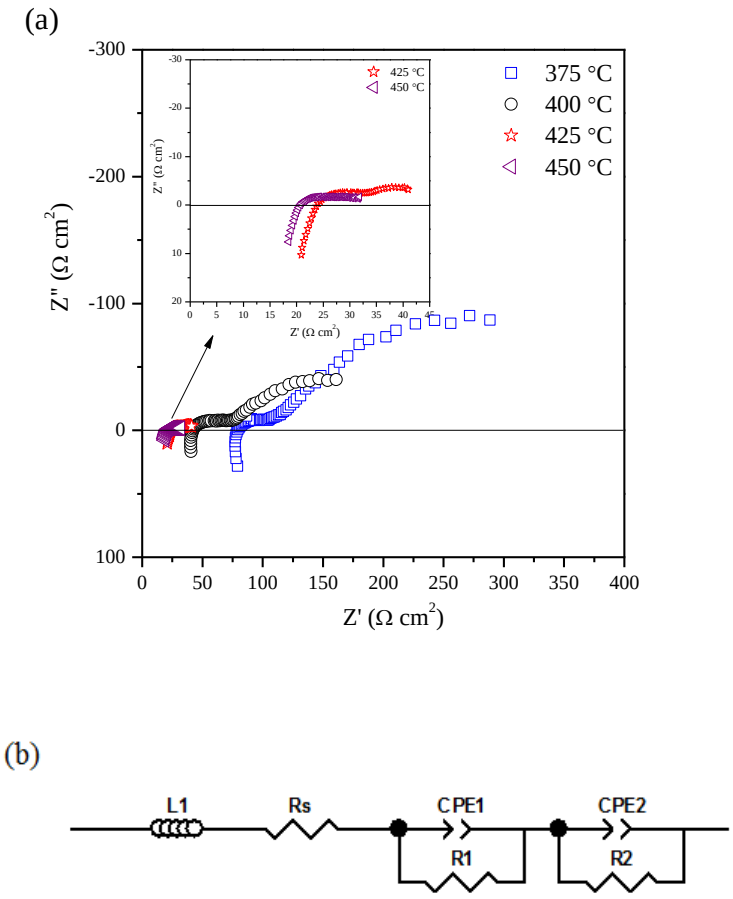

Figure 6. (a) Impedance spectra under open circuit condition of the cell based on CFo-CGDC composite cathode at 375-450 °C; (b) an equivalent circuit for the impedance data.

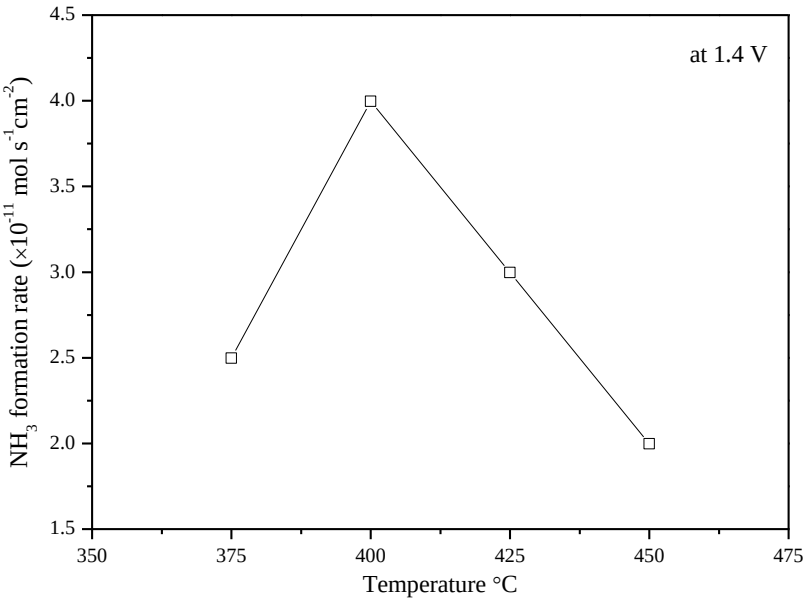

Figure 7. Dependence of the rate of ammonia formation on the operating temperature. The electrolytic cell was; air, SSCo-CGDC|CGDC-carbonate|CFO-CGDC, 3% H_2O-N_2.

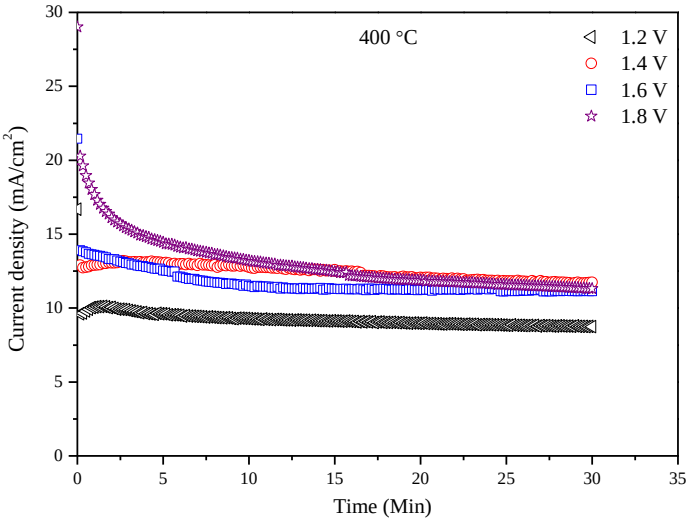

Figure 8. Electrolytic cell performance stability at 400 °C and under different voltages (1.2-1.8 V).The electrolytic cell was; air, SSCo-CGDC|CGDC-carbonate|CFO-CGDC, 3% H_2O-N_2.

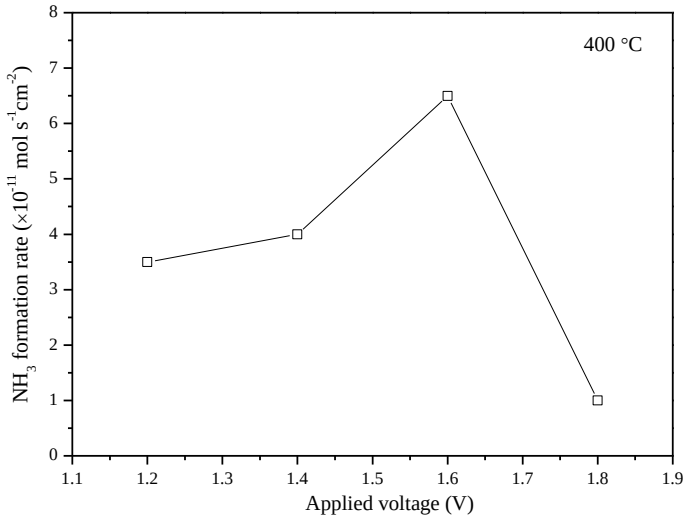

Figure 9. Dependence of the rate of ammonia formation on the applied voltage at 400 °C. The electrolytic cell was: air, SSCo-CGDC|CGDC-carbonate|CFO-CGDC, 3% H_2O-N_2.

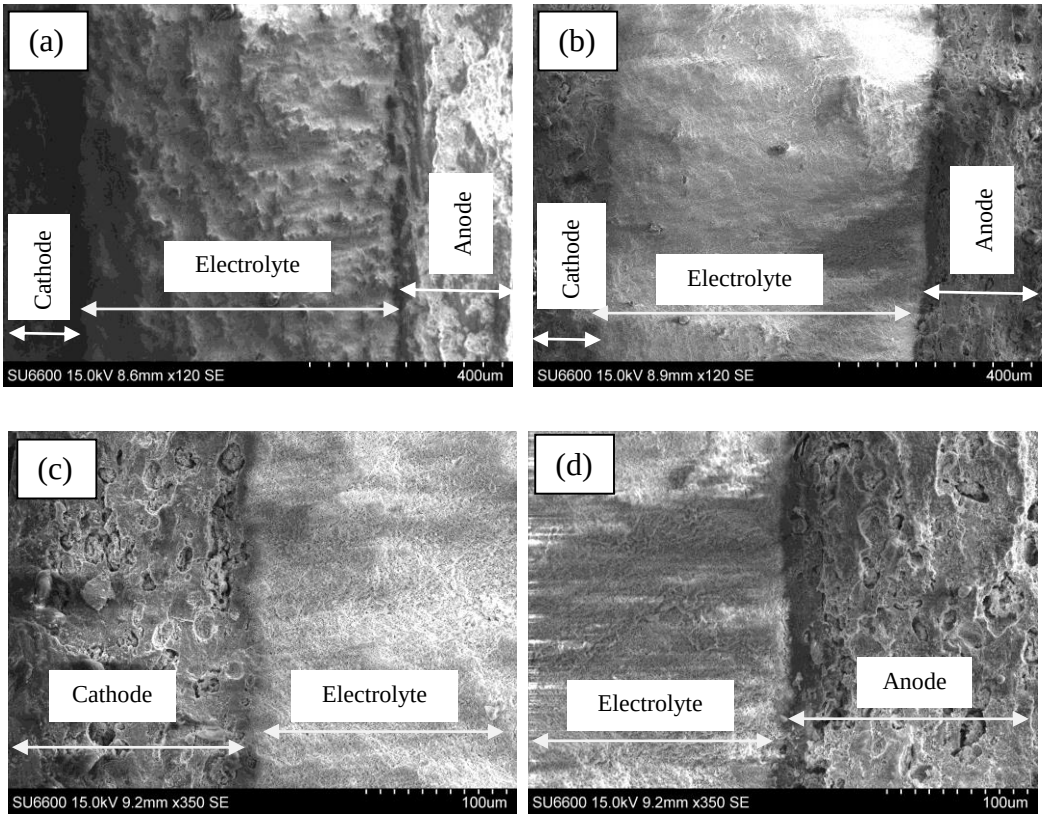

Figure 11. Cross-sectional scanning electron micrographs of the single cell. (a) before ammonia synthesis; (b) after ammonia synthesis experiments; (c) interface between cathode and electrolyte after ammonia synthesis experiments; (d) interface between electrolyte and anode after ammonia synthesis experiments.